Original Article

Transgenic Mouse Overexpressing Syntaxin-1A as a Diabetes Model

Patrick P.L. Lam,[1,2] Yuk-Man Leung,[1,2] Laura Sheu,[1,2] James Ellis,[3] Robert G. Tsushima,[1,2] Lucy R. Osborne,[1,4] and Herbert Y. Gaisano[1,2]

Soluble *N*-ethylmaleimide–sensitive factor (NSF) attachment protein receptor (SNARE) protein syntaxin-1A (STX-1A) plays a role not only in exocytosis, but also binds and regulates Ca^{2+} and K^+ (voltage-gated K^+ and ATP-sensitive K^+ channels) to influence the sequence of events leading to secretion. Islet levels of STX-1A and cognate SNARE proteins are reduced in type 2 diabetic rodents, suggesting their role in dysregulated insulin secretion contributing to the abnormal glucose homeostasis. We investigated the specific role of STX-1A in pancreatic β-cells by generating transgenic mice, which express a moderately increased level (~30% higher) of STX-1A in pancreatic islets (hereafter called STX-1A mice). The STX-1A mice displayed fasting hyperglycemia and a more sustained elevation of plasma glucose levels after an intraperitoneal glucose tolerance test, with correspondingly reduced plasma insulin levels. Surprisingly, β-cells from the STX-1A male mice also exhibited abnormal insulin tolerance. To unequivocally determine the β-cell secretory defects, we used single-cell analyses of exocytosis by patch clamp membrane capacitance measurements and ion channel recordings. Depolarization-evoked membrane capacitance increases were reduced in the STX-1A mouse islet β-cells. The STX-1A mouse also exhibited reduced currents through the Ca^{2+} channels but little change in the voltage-gated K^+ channel or ATP-sensitive K^+ channel. These results suggest that fluctuation of islet STX-1A levels in diabetes could influence the pathological and differential regulation of β-cell ion channels and the exocytotic machinery, collectively contributing to the impaired insulin secretion. *Diabetes* 54: 2744–2754, 2005

The soluble *N*-ethylmaleimide–sensitive factor (NSF) attachment protein receptor (SNARE) proteins are well known to mediate insulin exocytosis (1). In the islet β-cell, glucose entry generates an increase in ATP-to-ADP ratio, which closes the ATP-sensitive K^+ channels (K_{ATP} channels) [rev. in (2,3)]. This results in membrane depolarization, which activates and opens the L-type Ca^{2+} channel to allow Ca^{2+} influx. An increase in cytosolic Ca^{2+} would then trigger exocytosis of the docked and primed insulin granules. The voltage-gated K^+ (K_v) channel, specifically $K_v2.1$, is then activated, which causes membrane repolarization, resulting in closure of the Ca^{2+} channel that leads to a cessation of insulin secretion. SNARE proteins, particularly syntaxin-1A (STX-1A), have been shown to directly bind and regulate not only the L-type Ca^{2+} channels (4,5), but also K_{ATP} (6) and $K_v2.1$ channels (7,8) of the islet β-cells. This led to our broad hypothesis that these SNARE proteins could orchestrate the sequence of ionic and exocytic events leading to insulin secretion.

In type 2 diabetes rat models, including the Zucker *fa/fa* and Goto-Kakizaki (GK) rats, islet levels of STX-1A, along with its cognate SNARE partners (synaptosome-associated protein of 25 kDa [SNAP-25] and vesicle-associated membrane protein 2 [VAMP-2]) and associated proteins (Munc18a, Munc13–1) are severely reduced (9–11). In fact, real-time imaging of insulin exocytosis from GK rat islet β-cells showed reduced first-phase secretion, which is accountable in part by a reduced number of docked insulin granules (12). Such reduction must be at least contributed by the decreased levels of exocytic SNARE proteins. In fact, normoglycemic control of the GK rat resulted in the partial restoration in the islet levels of SNARE proteins and insulin secretion (10). Adenoviral gene transfer of STX-1A into the GK islets also restored insulin secretion (13); however, overexpression of STX-1A in normal islets (13) or insulinoma cell lines (14) actually reduced insulin secretion.

The genetic alteration of STX-1A levels might also contribute to the abnormal glucose homeostasis in human diabetes. In fact, an abnormal glucose metabolism was

From the [1]Department of Medicine, University of Toronto, Toronto, Canada; the [2]Department of Physiology, University of Toronto, Toronto, Canada; the [3]Program in Developmental Biology, Sick Kids Hospital, Toronto, Canada; and the [4]Department of Molecular and Medical Genetics, University of Toronto, Toronto, Canada.

Address correspondence and reprint requests to Herbert Y. Gaisano, MD, University of Toronto, Room 7226, Medical Science Building, 1 King's College Circle, Toronto, Ontario, Canada M5S 1A8. E-mail: herbert.gaisano@utoronto.ca. Or Lucy R. Osborne, PhD, University of Toronto, Room 7238, Medical Science Building, 1 King's College Circle, Toronto, Ontario, Canada M5S 1A8. E-mail: lucy.osborne@utoronto.ca.

Received for publication 23 November 2004 and accepted in revised form 7 June 2005.

P.P.L.L. and Y.-M.L. contributed equally to this work.

Cm, membrane capacitance; GST, glutathione S-transferase; IPGTT, intraperitoneal glucose tolerance test; K_{ATP} channel, ATP-sensitive K^+ channel; K_v channel, voltage-gated potassium channel; NSF, *N*-ethylmaleimide–sensitive factor; SNAP-25, synaptosome-associated protein of 25 kDa; SNARE, soluble NSF attachment protein receptor; STX-1A, syntaxin-1A; TEA, tetraethylammonium; VAMP-2, vesicle-associated membrane protein 2; WBS, Williams-Beuren syndrome.

recently reported in Williams-Beuren syndrome (WBS; OMIM 194050) (15), a multisystem developmental disorder caused by the hemizygous deletion of a 1.5-million–bp region of chromosome 7q11.23, which includes the STX-1A gene (16). Patients with WBS exhibit a variety of endocrine phenotypes, including transient hyperparathyroidism, hypercalcemia, and an increased incidence of diabetes (15). Of 20 adults with WBS (average age, 39 years) who underwent oral glucose tolerance testing, only two (10%) had normal glucose metabolism, with the remaining 90% having diabetes ($n = 3$), silent diabetes ($n = 6$), or impaired glucose tolerance ($n = 9$), according to criteria established by the Expert Committee on Diabetes (17).

Taken together, these studies suggest that the fluctuating levels of STX-1A in pancreatic islets occurring in health and in diabetes must have an exquisite control on the different components of secretion, including the exocytic machinery and membrane ion channels. In fact, diabetic islets seem to be particularly prone to fluctuations in the levels of SNARE proteins induced by the glycemic states (10). We have hypothesized that small perturbations of the levels of STX-1A in islet β-cells, either a small decrease or increase, could induce distinct effects on these different components of the insulin secretory machinery. To address this, we have generated a transgenic mouse that moderately overexpresses human STX-1A (by 30% of endogenous protein levels), with the anticipation that this slight increase in STX-1A might induce positive regulatory actions on the insulin secretory machinery. Because we used the human gene in its genomic context to generate transgenic lines, STX-1A protein is expressed in a tissue-specific manner that mimics that of the endogenous STX-1A protein. This allows us to examine which of the secretory components are more sensitive to this slight increase of STX-1A level and whether this would be sufficient to influence islet β-cell insulin exocytosis and glucose homeostasis. To our surprise, a small increase in islet STX-1A levels actually reduced insulin exocytosis sufficiently to induce glucose intolerance, and more surprisingly, the STX-1A male mice also exhibited abnormal insulin intolerance. We also show that the islet β-cell L-type Ca^{2+} channel was the most sensitive of the ion channels (compared with K_{ATP} and $K_v2.1$) to perturbation of STX-1A levels. It therefore appears that a slight overexpression of STX-1A could profoundly alter the many steps of insulin secretion, which would collectively contribute to the abnormal glucose homeostasis in diabetes.

RESEARCH DESIGN AND METHODS

Generation of STX-1A transgenic mice. A genomic cosmid LL07NC01-16g10 containing the entire human STX-1A gene was used. Cosmid DNA was prepared using Plasmid Maxi kits (Qiagen, Santa Clara, CA) and a 26-kilobase genomic fragment was excised from the cosmid backbone by digestion with *Eco*RI. The genomic fragment was recovered from 0.7% TAE agarose gel slices using dialysis and Elutip-d columns (Schleicher & Schuell, Mississauga, Canada) and resuspended in injection buffer (10 mmol/l Tris-HCl, pH 7.5, and 0.2 mmol/l EDTA) at 0.5–1 ng/μl. Injection was performed on fertilized FVB mouse eggs that were then transferred into recipient CD1 female animals as we previously described (18). Offspring were screened for integration of the transgene by PCR amplification of the human STX-1A 3′-untranslated region using the primers F, 5′-GTGAGTGTGCGTCTGTACGGG-3′, and R, 5′-TCAGGGTCACCTCTCCCCTAAC-3′. Cycles were performed as follows: 94°C for 5 min; 35 cycles of 94°C for 30 s, 60°C for 45 s, and 72°C for 30 s; and a final extension of 72°C for 10 min. The 291-bp product was resolved on a 3% agarose gel.

Determination of transgene copy number and expression analysis. Copy-number determination was performed using the EagleEye II (Stratagene, La Jolla, CA). Serial dilutions of the cosmid DNA representing different genome copy numbers of the transgene and genomic DNA from the transgenic lines were digested with *Eco*RI and *Bam*HI, resolved on 0.8% agarose gels, and transferred to a nylon membrane by Southern blotting. The 291-bp human-specific PCR product from the 3′-untranslated region of STX-1A was used as a hybridization probe. To assess transgene expression, the same primer pair was used for RT-PCR amplification of the human STX-1A transcript from total RNA. RNA was extracted from tissues using TRIzol Reagent and reverse transcribed using SuperScript III (Invitrogen, Carlsbad, CA). A control amplification of reverse transcription reaction without the addition of SuperScript III was used to ensure there was no DNA contamination.

DNA construct and recombinant glutathione S-transferase proteins. The construct pGEX-4T-1-STX-1A, used for generating glutathione S-transferase (GST)-STX-1A protein, has been reported previously (7). GST-STX-1A protein expression and purification were performed following the instructions of Amersham Biosciences. Before elution of the GST fusion protein from glutathione agarose beads, STX-1A protein was obtained by cleavage of GST-STX-1A with thrombin to remove the GST (Sigma, St. Louis, MO)

Intraperitoneal glucose tolerance test IPGTT. Mice were fasted overnight between 12 and 16 h before experimental procedures were carried out to assay for glucose tolerance after fasting and subsequently to glucose challenge. Their body weights before and after fasting were measured and recorded to the nearest gram unit. A drop of tail blood was taken by introducing a 23.5-gauge needle puncture and assayed for basal glucose levels ($t = 0$) using the OneTouch glucose meter (Lifescan, Vancouver, Canada). A 1–2 mg D-glucose/kg fasting body wt dose of glucose was injected into the intraperitoneum of the mice, and tail blood was taken at $t = 15$, 30, 45, 60, 90, and 120 min postinjection for glucose measurement. The mice were allowed to recover for 2 weeks before the next scheduled experiment. These and all experiments below were carried out in accordance with the Canadian Council for Animal Care guidelines and were approved by the University of Toronto Animal Care Committee.

Determination of serum insulin during IPGTT. Mice were restrained in a 50-ml syringe tube (BD Biosciences, Toronto, Canada), with a punctured hole at the bottom of the tube to allow for continuous airflow. The hind leg was extended and fixed by holding the fold of skin between the tail and thigh. Leg hairs were shaved using a sterile blade until the saphenous vein was apparent for visualization. A 23.5-gauge needle was then used to puncture the saphenous vein, and ~50 μl of blood was collected into a Microvette untreated with heparin (Sarstedt, Toronto, Canada), recorded as $t = 0$ min (basal level). During the IPGTT, blood samples were obtained at $t = 10$, 30, and 120 min. The flow of blood had been optimized for collection by coating the surface of the epidermis with a thin film of Vaseline to prevent clotting and coagulation. Blood was allowed to stand at room temperature for at least 20 min to allow clotting. Serum was then separated by spinning down the plasma at 4°C, 8,000–10,000 rpm. Serum insulin levels were then assayed using the RIA Ultrasensitive Insulin kit (Linco Research, St. Charles, MO) or the ELISA (Crystal Chem, Chicago, IL).

Intraperitoneal insulin tolerance test. Mice were fasted for 5 h before experimental procedures were carried out to assay for insulin tolerance after fasting. Their body weights before and after fasting were measured and recorded to the nearest gram unit. A drop of tail blood was taken by introducing a 23.5-gauge needle puncture, and assayed for basal glucose levels ($t = 0$ min) using the OneTouch glucose meter (Lifescan). A 0.25–0.45 units insulin/kg fasting body wt injection of a short-acting human biosynthetic insulin (Novo Nordisk, Toronto, Canada) was injected into the intraperitoneum of the mice, and tail blood was taken at $t = 15$, 30, 45, 60, 90, and 120 min for insulin measurement. The mice were allowed to recover for 2 weeks before the next scheduled experiment.

Immunoblotting. Electrophoretic separations of proteins by SDS-PAGE and immunoblotting were performed as previously described (6,7). The mouse islets were solubilized in sample buffer (with 2% SDS) and boiled for 5 min. Because the size and quality of islets can vary, particularly in diabetic rats, extra care was taken to ensure accurate protein loading. First, the protein quality and quantity of each islet sample were determined by a modified Lowry's method. Second, equal protein loading of these islet samples was confirmed by uniform Coomassie Blue staining of all lanes and in all gels. From each sample, 20 μg protein was loaded and separated on a 15% polyacrylamide gel. The proteins were then transferred to nitrocellulose membranes and incubated with the primary mouse monoclonal or rabbit polyclonal antibodies: STX-1A monoclonal antibody, 1:1,000 dilution (Sigma); SNAP-25 monoclonal antibody, 1:1,000 (SMI-25; Sternberger Monoclonal, Lutherville, MD); VAMP-2 polyclonal antibody, 1:1,000 (9,10); nSec1/Munc18a monoclonal antibody, 1:1,000 (BD Transduction Laboratories, San Jose, CA);

and mouse anti-actin antibody, 1:20,000 (Roche Molecular Biochemicals, Québec, Canada), all for 1.5–2 h at room temperature. These primary antibodies were then detected with appropriate secondary antibodies and visualized by chemiluminescence (Pierce Chemical, Rockford, IL) and exposure of the filters to Kodak BMR film (Eastman Kodak, Rochester, NY) for 1 s to 10 min. For quantification of the SNARE protein signals, several film exposures of the blots were scanned and analyzed using NIH Image (version 1.61).

Recording of K^+ and Ca^{2+} currents. Mouse β-cells were voltage-clamped in the whole-cell configuration using an EPC-9 amplifier and Pulse software (HEKA Electronik, Lambrecht, Germany) as we previously described (6,7). β-Cells were identified by their characteristic display of substantial Na^+ currents only at very negative (−120 mV) holding potential. Recording pipettes were pulled from 1.5-mm borosilicate glass capillary tubes (World Precision Instruments, Sarasota, FL) using a programmable micropipette puller (Sutter Instrument, Novato, CA). Pipettes were then heat-polished, and tip resistances ranged from 3.5 to 5 MΩ when filled with intracellular solutions. The intracellular solution for K_v current measurements contained 140 mmol/l KCl, 1 mmol/l $MgCl_2$, 1 mmol/l EGTA, 10 mmol/l HEPES, and 5 mmol/l MgATP (pH 7.25 adjusted with KOH). For K_{ATP} current measurements, the intracellular solution was the same as above except that MgATP was reduced to 0.3 mmol/l to allow K_{ATP} channel opening. The intracellular solution for Ca^{2+} current measurement contained 120 mmol/l CsCl, 20 mmol/l tetraethylammonium (TEA)-Cl, 1 mmol/l $MgCl_2$, 1 mmol/l EGTA, 10 mmol/l HEPES, and 5 mmol/l MgATP (pH 7.25 adjusted with CsOH). The bath solution for K_v and K_{ATP} current measurements contained 140 mmol/l NaCl, 4 mmol/l KCl, 1 mmol/l $MgCl_2$, 2 mmol/l $CaCl_2$, 2 mmol/l D-glucose, and 10 mmol/l HEPES (pH 7.3 adjusted with NaOH). The bath solution for Ca^{2+} current measurement was the same as above except that 20 mmol/l TEA-Cl was also added, and the concentration of $CaCl_2$ was increased to 10 mmol/l. After the whole-cell configuration was established, the cell was held at −70 mV and subject to various experimental protocols as detailed in RESULTS and in the figure legends. All experiments were performed at room temperature (~22°C).

Simultaneous measurement of capacitance and Ca^{2+} currents. Recording electrodes were coated with orthodontic wax (Butler, Guelph, ON, Canada) close to the tips and heat-polished. Resistances ranged from 3.5 to 5 MΩ when pipettes were filled with the intracellular solution, which contained 120 mmol/l CsCl, 20 mmol/l TEA-Cl, 1 mmol/l $MgCl_2$, 0.1 mmol/l EGTA, 10 mmol/l HEPES, 0.1 mmol/l cAMP, and 5 mmol/l MgATP (pH 7.25 adjusted with CsOH). The extracellular solution contained 140 mmol/l NaCl, 4 mmol/l KCl, 1 mmol/l $MgCl_2$, 10 mmol/l $CaCl_2$, 20 mmol/l TEA, 2 mmol/l D-glucose, and 10 mmol/l HEPES (pH 7.3 adjusted with NaOH). Cell capacitance was estimated by the Lindau-Neher technique, implementing the "Sine + DC" feature of the Lock-in module (40 mV peak to peak and a frequency of 500 Hz) in the standard whole-cell configuration. Recordings were conducted using an EPC9 patch clamp amplifier and Pulse software. Exocytic events were elicited by a train of eight 500-ms depolarizing pulses (1-Hz stimulation frequency) from −70 to 0 mV. The experimental temperature was set at 28–30°C.

Statistics. Results are presented as means ± SE. ANOVA was used for multiple group comparisons, and statistical significance was determined by Student's t test. A P value <0.05 was considered statistically significant.

RESULTS

Generation of transgenic mice expressing human STX-1A. Four mouse lines were born that had integrated the genomic DNA fragment and all were able to transmit the transgene through their germline. Of these four lines, three (designated A11, B14, and B15) were found to express human STX-1A mRNA as evidenced by RT-PCR amplification of human-specific STX-1A transcript from brain total RNA. Copy number determination was performed, and the lines were calculated to contain four, two, and one copy of the human genomic fragment, respectively (Fig. 1*A*). Expression analysis demonstrated an abundant human STX-1A message in the brains of all three lines, with barely detectable levels present in the liver, kidney, lung, and intestine (data not shown), suggesting that the transgene was expressed under the control of its endogenous regulatory elements. Irrespective of their genetic background, the STX-1A mice were indistinguishable from their control littermates with respect to their appearance, growth, and fertility in the animal facility. The gross histology of the STX-1A mice brain (data not shown) and pancreas (Fig. 1*B*, islets indicated by arrows) were normal. We did not observe any premature deaths recorded at birth for all lines of the STX-1A mice, and some of these mice were allowed to live past 52 weeks of age and remained healthy.

However, when we determined the basal fasting glucose levels at 1 year of age (Fig. 1*C*), the B14 STX-1A mouse line glucose levels were higher (7.50 ± 0.12 mmol/l, $n = 9$) when compared with wild-type mice (5.30 ± 0.32 mmol/l, $n = 6$, $P < 0.01$), whereas the A11 STX-1A mouse line exhibited even higher basal glucose levels (8.20 ± 0.29 mmol/l, $n = 5$, $P < 0.01$). The basal glucose levels at 12 weeks of age were also similarly higher in the A11 (7.20 ± 0.46 mmol/l, $n = 4$) and B14 (6.60 ± 1.44 mmol/l, $n = 3$) lines compared with wild-type littermates (4.40 ± 0.75 mmol/l, $n = 6$, $P < 0.01$).

Both the A11 and B14 lines also showed increased pancreatic islet expression of STX-1A protein (see below), which along with the corresponding increase in basal glucose levels (B15 line not tested), indicated that the STX-1A transgene was exerting an effect that was independent of the site of insertion in the mouse genome. Because the A11 line had higher islet STX-1A protein levels and more consistently exhibited higher baseline glucose levels, all subsequent studies on glucose homeostasis and islet functions were performed on the A11 line alone. At 18 weeks of age, when these mice were of optimal size for the in vivo studies and islet isolation, we examined their weights. The weights of the STX-1A mice (A11 line) and wild-type mice were not significantly different for either males (STX-1A, 30.00 ± 2.00 g vs. wild type, 29.00 ± 1.00 g; $n = 14$) or females (STX-1A, 26.00 ± 1.00 g vs. wild type, 27.00 ± 1.00 g; $n = 14$).

Expression of human STX-1A is confirmed in the pancreatic islets. The basal hyperglycemia in the STX-1A mice suggested a possible insulin secretory defect of the pancreatic islets, in which STX-1A is known to be abundant and plays important roles in insulin secretion. Because the human STX-1A transgene expression is under its own transcriptional control, we expected to find corresponding changes in the STX-1A levels in the islets of the STX-1A mouse pancreas. Figure 2*A* shows a representative experiment of the actual blots of the levels of the indicated proteins of the isolated islets of a single wild-type and STX-1A mouse. Figure 2*B* shows the densitometry quantification of three to four independent islet isolations, represented as percentages of the wild-type littermate's signals. Islets from the A11 line showed a 28.38 ± 8.09% ($P < 0.05$) increase in STX-1A protein expression, compared with those from the wild-type mice, whereas the B14 lines showed a small increase of only 5–10% (data not shown). The relatively low levels of STX-1A protein expression in each line are likely due to differences between humans and mice in the specificity of factors involved in the regulation of transcription or translation. We then examined whether this increase in STX-1A expression in the A11 STX-1A mouse islets might influence the expression of the cognate SNARE proteins (SNAP-25 and VAMP-2) and major STX-1A–interacting protein Munc18a (19,20). Compared with wild-type littermate islets, the A11 STX-1A mice islet VAMP-2 and SNAP-25 levels were un-

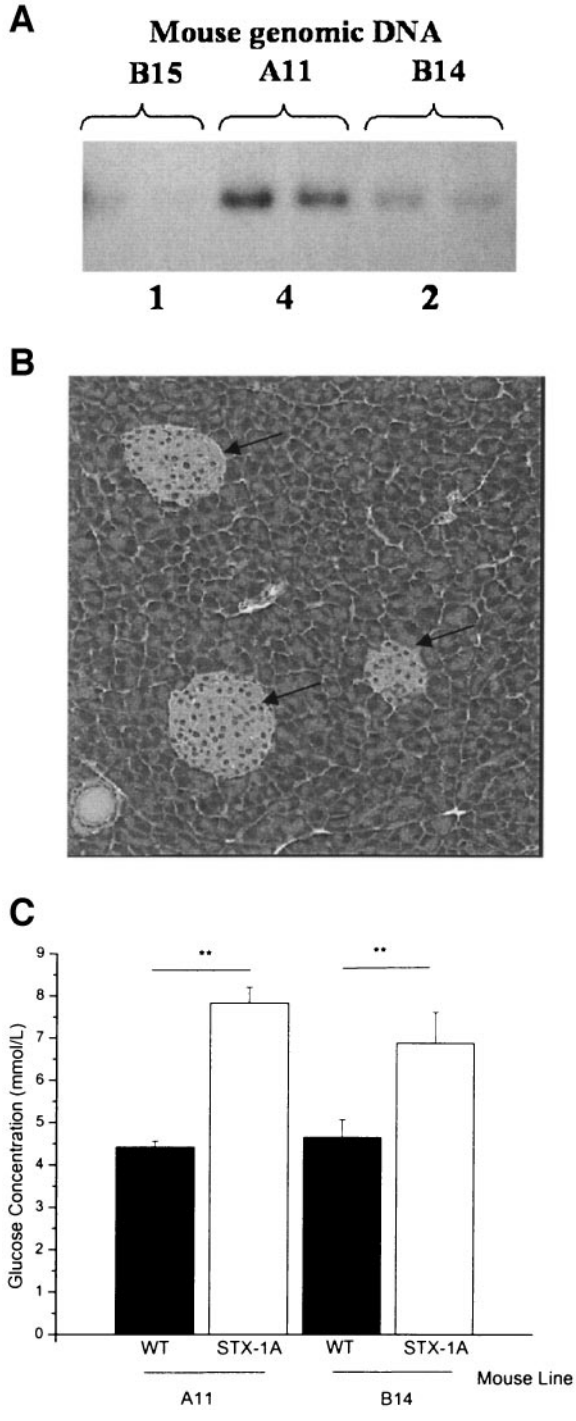

FIG. 1. Generation of transgenic mice expressing human STX-1A. *A*: Human STX-1A transgene copy number of the STX-1A mouse lines (A11, B14, and B15). Replicate samples from two mice of each line are shown. *B*: STX-1A mice have normal pancreatic histology (hematoxylin and eosin stain). Arrows point to the islets. *C*: Basal serum glucose levels of the STX-1A A11 and B14 mouse lines at 1 year of age. Values are means ± SE (wild-type [WT] mice, $n = 6$; B14 STX-1A mice, $n = 9$; A11 STX-1A mice, $n = 5$). **$P < 0.01$ compared with wild-type littermates.

changed. Surprisingly, in the STX-1A mice (A11), islet Munc18a levels showed a paradoxical reduction in protein expression by 30.84 ± 14.14% ($P < 0.05$) compared with those from the wild-type mice. The expression levels of actin served as an indicator of equal protein loading. We also determined the insulin content of the A11 STX-1A mice islets (by radioimmunoassay), which was not significantly different from the wild-type littermates in both males (STX-1A, 1.87 ± 0.29 ng/ml vs. wild type, 2.02 ± 0.53 ng/ml) and females (STX-1A, 1.72 ± 0.41 ng/ml vs. wild type, 1.92 ± 0.13 ng/ml).

STX-1A mice exhibit glucose intolerance during IPGTT. We had hypothesized that the slight increase in STX-1A levels in the islets might be sufficient to induce an abnormality in glucose homeostasis, which we examined by IPGTT. As shown in Fig. 3, both male and female groups of STX-1A mice exhibited significantly higher levels of fasting blood glucose levels compared with control littermates. This was more evident in the STX-1A male mice (STX-1A, 8.12 ± 0.26 mmol/l, vs. wild type, 7.33 ± 0.14 mmol/l, $P < 0.05$) than the STX-1A female mice (STX-1A, 7.88 ± 0.22 mmol/l, vs. wild type, 6.54 ± 0.04 mmol/l, $P < 0.05$). After the intraperitoneal glucose injection, the serum glucose rise in both male and female groups of the STX-1A mice were significantly higher than the control littermates but were observed to be more severe in the male STX-1A mice. At 30 min, peak serum glucose levels for STX-1A male mice were 18.80 ± 0.36 mmol/l, compared with wild-type male littermates of 13.10 ± 0.15 mmol/l ($P < 0.05$). At 30 min, serum glucose levels for STX-1A female mice were also measured to be at 15.02 ± 0.32 mmol/l compared with wild-type female littermates of 13.28 ± 0.42 mmol/l ($P < 0.05$). This abnormal glucose homeostasis was sustained up to 120 min of serum glucose recording; the STX-1A male and female mice had a recorded glucose level of 13.23 ± 0.31 and 10.82 ± 0.54 mmol/l, respectively, which were significantly higher than their control littermates of 8.60 ± 0.28 and 8.00 ± 0.37 mmol/l ($P < 0.05$), respectively. These results taken together suggest that the STX-1A mice exhibited glucose intolerance that was more severe in males compared with females.

STX-1A mice release less insulin during IPGTT. The glucose intolerance exhibited by the STX-1A mice during the IPGTT can be due to either reduced insulin release into the circulation or the resistance of peripheral tissues to the insulin action. We first examined the insulin that is released into the bloodstream during the IPGTT (Fig. 4*A*). Of note, the fasting serum levels were already significantly lower in both STX-1A male (0.30 ± 0.02 ng/ml) and female (0.40 ± 0.02 ng/ml) mice compared with the control male (0.42 ± 0.05 ng/ml, $P < 0.01$) and female (0.56 ± 0.03 ng/ml, $P < 0.05$) littermates, which may in part account for the differences in fasting blood glucose (in Fig. 2). Serum insulin levels were determined at 10, 30, and 120 min after glucose stimulation. In Fig. 4*B*, we determined the integrated net rise in insulin levels above the basal fasting levels encompassed by these time points as the area under the curve. Here, STX-1A male and female mice had a net release of insulin of 86.40 ± 0.20 ng/ml × 120 min and 89.70 ± 1.60 ng/ml × 120 min, respectively, which were significantly lower than the wild-type male (125.20 ± 2.60 ng/ml × 120 min, $P < 0.01$) and female littermates (108.40 ± 3.30 ng/ml × 120 min, $P < 0.05$). Again, it appears that the male STX-1A mice had a more severe insulin secretory defect (~31% reduction compared with wild-type littermates) than the female STX-1A mice (~17% reduction compared with wild-type littermates).

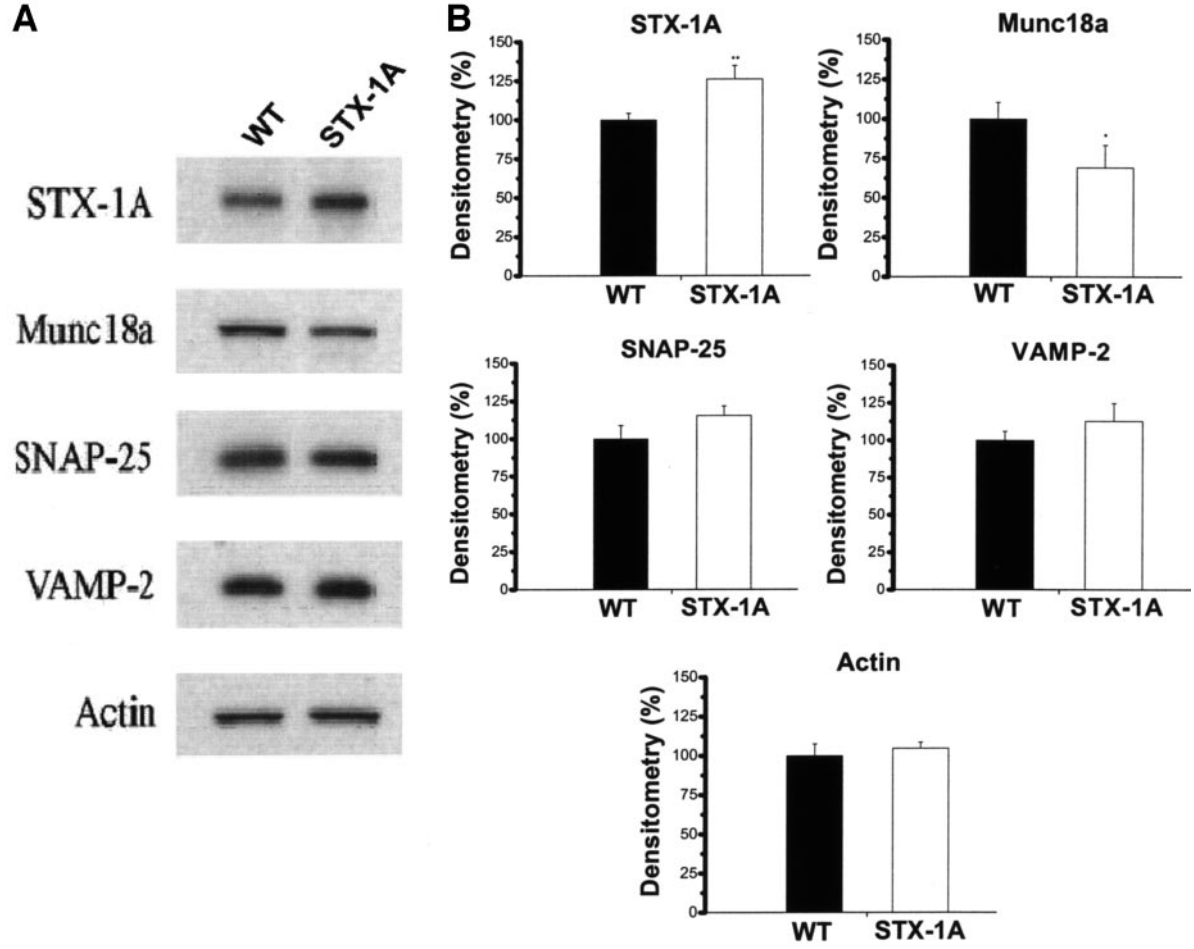

FIG. 2. Pancreatic islet levels of SNARE and STX-1A–activating proteins in the A11 STX-1A mouse line (four copies of the STX-1A transgene; Fig. 1A) and control wild-type (WT) littermates. Pancreatic islet samples (~20 μg protein per lane) were resolved on a 15% SDS-PAGE, and the separated proteins were identified by the indicated antibodies. *A*: A representative experiment of islets isolated from one set of wild-type and STX-1A mice. *B*: The densitometry performed on each of three to four independent islet isolations and presented as a percentage of the signals of the wild-type littermate. **P* and ***P* are <0.05 compared with wild-type littermates.

STX-1A male mice exhibit insulin resistance. We then examined whether the abnormal glucose homeostasis in the STX-1A mice could be contributed by the resistance of peripheral tissues to insulin action by performing the intraperitoneal insulin tolerance test. We predicted that insulin sensitivity would not be affected in the STX-1A mice because STX-1A is not a dominant exocytotic protein in insulin sensitive tissues (fat, muscle, and liver) (21). The serum glucose incursion in the STX-1A mice would be expected to parallel the control littermates in their response to an insulin challenge. Again, and as expected, the fasting glucose levels were higher in the STX-1A male and female mice (Fig. 5) compared with their control littermates. The glucose sensitivity to the insulin challenge was very similar for the female mice. Specifically, the maximal reduction in blood glucose levels (difference between time 0 and at 40 min after intraperitoneal insulin injection) were 2.94 ± 0.27 and 3.50 ± 0.11 mmol/l ($P = 0.19$), and the corresponding rates of glucose reduction were 0.069 and 0.079 mmol · l^{-1} · min^{-1}, respectively, for the female STX-1A and wild-type littermates. The male wild-type littermates exhibited a similar maximal reduction of 3.33 ± 0.03 mmol/l, and a rate of reduction of 0.074 mmol · l^{-1} · min^{-1}. But surprisingly, the STX-1A male mice exhibited insulin resistance with a maximal reduction in glucose levels of 1.98 ± 0.06 mmol/l ($P < 0.01$ compared with wild-type males), with a corresponding reduced rate of glucose reduction of 0.063 mmol · l^{-1} · min^{-1}, and that was preceded by an initial lag.

STX-1A mouse islet β-cells exhibit reduced exocytosis and Ca^{2+} currents. The abnormal glucose homeostasis (Fig. 3) in these STX-1A mice is therefore largely contributed by the insulin secretory deficiency. However, there seems to be a contribution by some insulin insensitivity of the peripheral tissues, at least in the male STX-1A mice (Fig. 5). To distinguish and examine the direct contribution of islet β-cell insulin secretory defect in the STX-1A mice, we used patch clamp membrane capacitance (Cm) measurements of single islet β-cells. As shown in Fig. 6*A*, top, serial depolarizations triggered substantial exocytosis in the control mouse β-cell. This depolarization protocol would release the insulin granules from the primed immediately releasable pool (first two to three pulses) as well as mobilize granules from the reserve pool to refill the releasable pool (subsequent pulses) (2). A massive Ca^{2+} current triggered by depolarization to 0 mV was simultaneously observed in this same cell (Fig. 6*A*, bottom). The increases in Cm in the STX-1A mouse β-cells were attenuated in both the first two and later pulses (Fig. 6*B*, top). This was also accompanied by a substantial

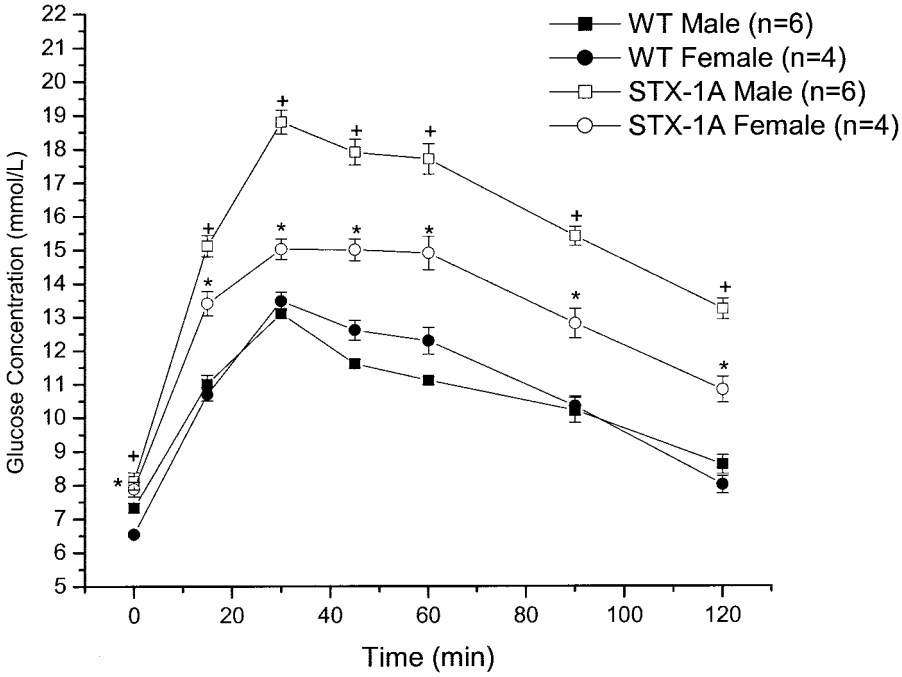

FIG. 3. STX-1A mice exhibit fasting hyperglycemia and sustained hyperglycemia during an IPGTT compared with wild-type (WT) littermates. All values are means ± SE from six male mice per group and four female mice per group. +P < 0.05 for male and *P < 0.05 for female STX-1A mice vs. wild-type mice.

reduction in Ca^{2+} influx (Fig. 6*B*, bottom). Results are summarized in Fig. 6*C* and *D*, which show that exocytosis and Ca^{2+} currents were concomitantly and significantly reduced in STX-1A mouse β-cells. These results suggest that STX-1A overexpression caused a major impairment in both the initial size of primed releasable pool of insulin granules and the subsequent mobilization of insulin granules from the reserve pool to the releasable pool. STX-1A directly binds and inhibits islet β-cell Ca^{2+} channels, and in fact, STX-1A was postulated to tether the insulin granules to the sparse L-type Ca^{2+} channels to more tightly couple Ca^{2+} channel opening (and Ca^{2+} influx) to exocytosis (22,23). Our results therefore also suggest that the reduced exocytosis in STX-1A mouse β-cells is attributed at least in part to the reduced Ca^{2+} influx through plasma membrane voltage-dependent Ca^{2+} channels.

STX-1A mouse islet β-cells exhibit reduced Ca^{2+} channel activity. In Fig. 7*A* and *B*, we examined the voltage-dependent Ca^{2+} currents in greater detail in control and STX-1A mice independently of the Cm. Results are summarized in Fig. 7*C*, which shows the peak Ca^{2+} currents plotted against membrane potential. Inward Ca^{2+} currents were triggered when the β-cell was depolarized to ≥ -30 mV, indicating that the Ca^{2+} currents were through high-voltage–activated Ca^{2+} channels (L-, N-type) but not low-voltage–activated Ca^{2+} channels (T-type, threshold of opening is ~ -50 mV). Current density was significantly reduced by ~30% in the STX-1A mouse group. Note that the reduction of Ca^{2+} currents occur within the physiological depolarizing range (-10 mV).

STX-1A mouse islet β-cell K_v and K_{ATP} channel activities were similar to wild-type mice. We had previously observed that a large excess of STX-1A, whether through dialysis of the STX-1A protein into rat islet β-cells or by overexpression of STX-1A into K_v2.1-expressing HEK cells, inhibited K_v2.1 channels (7,8). We therefore examined whether the slight overexpression of STX-1A in the STX-1A mouse β-cells might similarly reduce the K_v channel activities. Results in Fig. 8*A* show that the K_v channel activities in STX-1A mouse β-cells were only marginally and insignificantly reduced (upper and middle traces). This would suggest that the β-cell K_v2.1 channels are less sensitive to STX-1A than the Ca^{2+} channels. In support, dialysis of excess STX-1A protein (1 μmol/l) into the STX-1A islet β-cells was able to inhibit the K_v currents as we had previously reported (Fig. 8*A*, bottom trace) (7). Results are summarized in Fig. 8*B*. In a recent report, we also showed that in rat β-cells and the HIT β-cell line, dialyzing excess STX-1A proteins strongly inhibited K_{ATP} currents (6,24). We therefore proceeded to compare the K_{ATP} current density in control and STX-1A mouse β-cells, which also did not show a significant change in islet β-cell K_{ATP} current density between the control and STX-1A mouse groups (data not shown). It therefore appears that these islet β-cell K^+ channels are less sensitive to the small increase in islet β-cell STX-1A levels (30%, in Fig. 2) than the L-type Ca^{2+} channels, indicating that these K^+ channels are less functionally coupled to STX-1A than the Ca^{2+} channels.

DISCUSSION

The results from this work demonstrate that small fluctuations of STX-1A levels are sufficient to induce profound changes on the function of the secretory components controlling secretion. It seems that out of the membrane ion channels involved in secretion, the Ca^{2+} channel is the most tightly coupled functionally to STX-1A, and therefore it is sensitive to even a slightly higher level of STX-1A. In support, we found that membrane depolarization caused a concomitant reduction of exocytosis (by Cm) and Ca^{2+} current in the STX-1A islet β-cells. STX-1A alone inhibits Ca^{2+} channels (25), but in the presence of SNAP-25, it would then exhibit a positive regulatory action (25). Therefore, the stoichiometry of cognate SNARE proteins, which was perturbed in the STX-1A islets, is important not only for the exocytic machinery, but also for the mem-

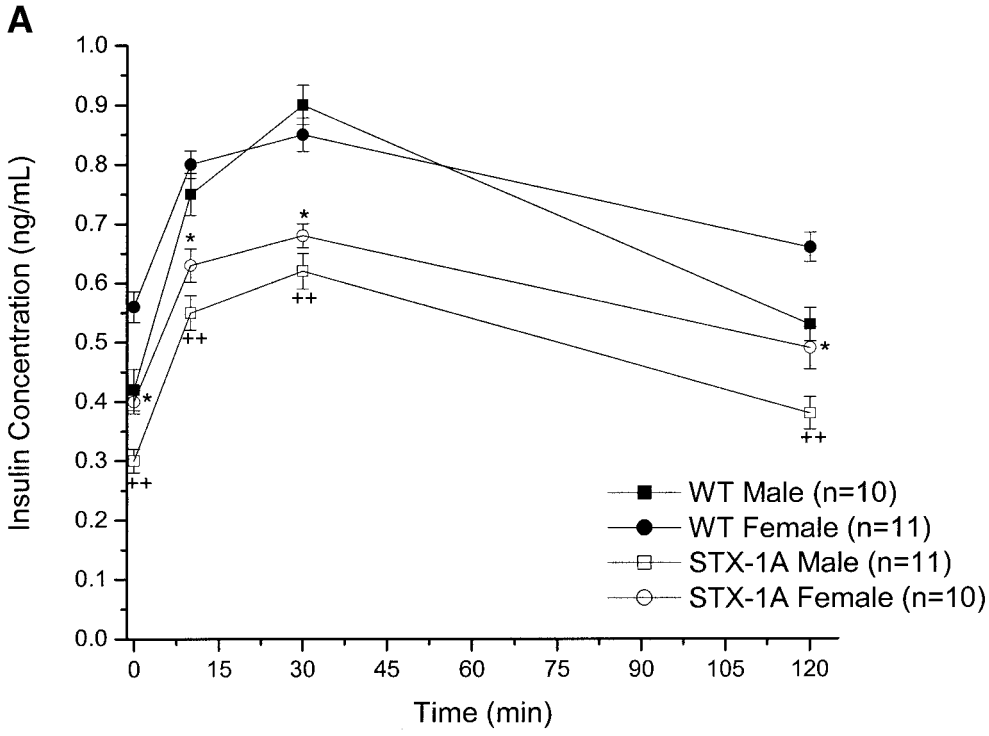

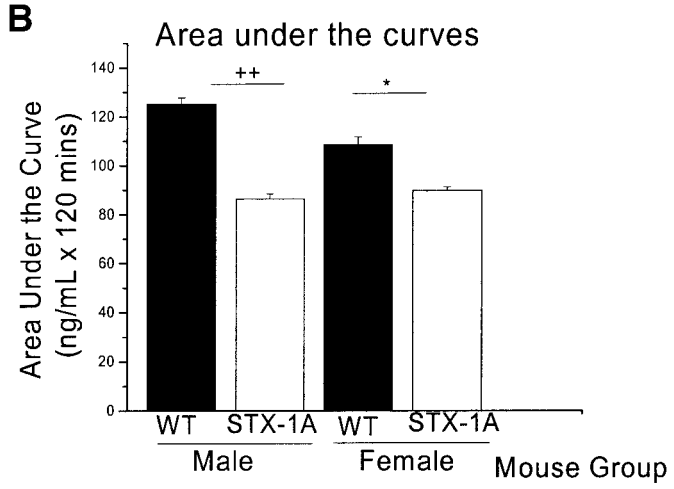

FIG. 4. STX-1A mice exhibit decreased insulin secretion in vivo during the IPGTT. *A*: Assessment of insulin secretion after glucose challenge during IPGTT shows a reduction in STX-1A mice versus wild-type (WT) littermates. All values are means ± SE from 11 male STX-1A mice and female wild-type mice and 10 male wild-type mice and female STX-1A mice. ++*P* < 0.01 for male and **P* < 0.05 for female STX-1A mice vs. wild-type mice. *B*: Net glucose-mediated insulin-release above basal levels quantified by the integration of the area under the curve. All values are means ± SE. ++*P* < 0.01; **P* < 0.05.

brane ion channels, to enable the normal functioning and regulation of these channels. The overexpressed human STX-1A differs from the host mouse STX-1A by just three amino acid residues located at the COOH terminus, including amino acid 278: V (human) versus I (mouse); amino acid 283: V (mouse) versus I (human); and the very COOH-terminal amino acid 288: A (human) versus G (mouse). These substitutions are small, nonpolar, and hydrophobic conserved residues, only one of which is in the transmembrane domain, with the other two sticking out into the extracellular domain, and which are therefore not expected to exhibit different actions on exocytosis or on the membrane ion channels. Although STX-1A and SNAP-25, acting as a complex, are also important for regulating islet β-cell $K_v2.1$ channel (26), this channel appears to be less sensitive to the slight increase in STX-1A levels. Nonetheless, the subsequent addition of excess exogenous STX-1A protein could then inhibit the K_v currents of the STX-1A islet β-cells. We also did not observe a significant effect on the K_{ATP} channels of the STX-1A islet β-cells. However, STX-1A levels in the islets of type 2 diabetic rodent models are reduced by >50% (10,11), and those levels become even further reduced with prolonged hyperglycemia (10). Such low levels of the STX-1A could then adversely influence these K^+ channels. This could contribute to the abnormal islet β-cell K_{ATP} channel function and its reduced glucose sensitivity in the diabetic GK rats (27).

The elevated STX-1A levels can certainly also affect exocytosis per se, because STX-1A is one of three minimal components (SNAP-25 and VAMP-2 being the other two) that comprise the exocytic machinery (19). Interestingly, we noted a ~30% reduction in the islet levels of Munc18a in the STX-1A mice. Munc18a plays an important role in insulin exocytosis (20), specifically by activating STX-1A into an "open" conformation, which can then bind the cognate SNARE proteins to consummate exocytosis (19,28,29). The reduced levels of Munc18a could result in

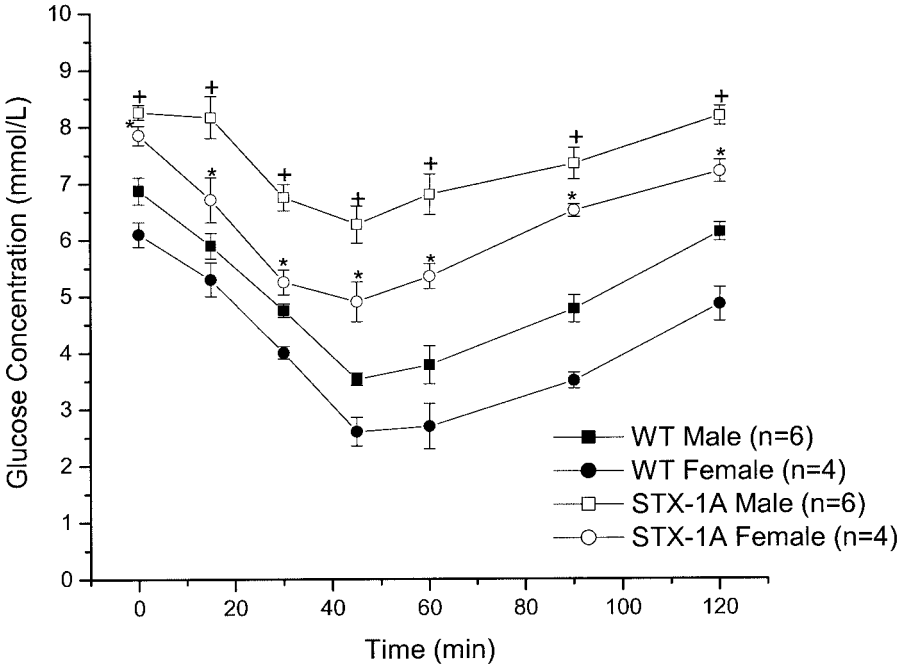

FIG. 5. STX-1A mice exhibit insulin resistance during intraperitoneal insulin tolerance test compared with wild-type (WT) littermates. All values are means ± SE from six male mice per group and four female mice per group. For each mouse, multiple IPGTTs of at least four per mouse were carried out, and the mean of these multiple IPGTTs was considered to be $n = 1$. $+P < 0.05$ for male and $*P < 0.05$ for female STX-1A mice vs. the wild-type mice.

a reduced efficiency of converting the moderate excess of STX-1A into its open form, which is required to prime secretory granules, and thereby contribute to the reduced size of the primed releasable pool and the less efficient mobilization of insulin granules to the releasable pool as observed in our study. Munc18a however has not been demonstrated to directly affect Ca^{2+} channels. The open conformation of STX-1A regulates β-cell $K_v2.1$ and K_{ATP} channels more effectively than wild-type STX-1A (8,24), but presumably, the small changes in Munc18a levels on STX-1A in the STX-1A mouse islets may not be sufficient to severely perturb STX-1A actions on these K^+ channels. Why the islet Munc18a levels in STX-1A pancreatic islets are reduced is not clear, but it could be the effects of the overexpressed STX-1A on Munc18a synthesis or stability.

The abnormal glucose homeostasis in the STX-1A–overexpressing male mice was due not only to abnormal insulin secretion, but surprisingly, we also found reduced insulin sensitivity of the peripheral tissues. Glucose transport via Glut4 in the insulin-sensitive tissues, including fat and muscles, is also regulated by SNARE proteins (21); however, the primary syntaxin that regulates Glut4 transport is STX-4 (along with SNAP-23 and VAMP-2) and not STX-1A (21). Therefore, the defective insulin sensitivity of

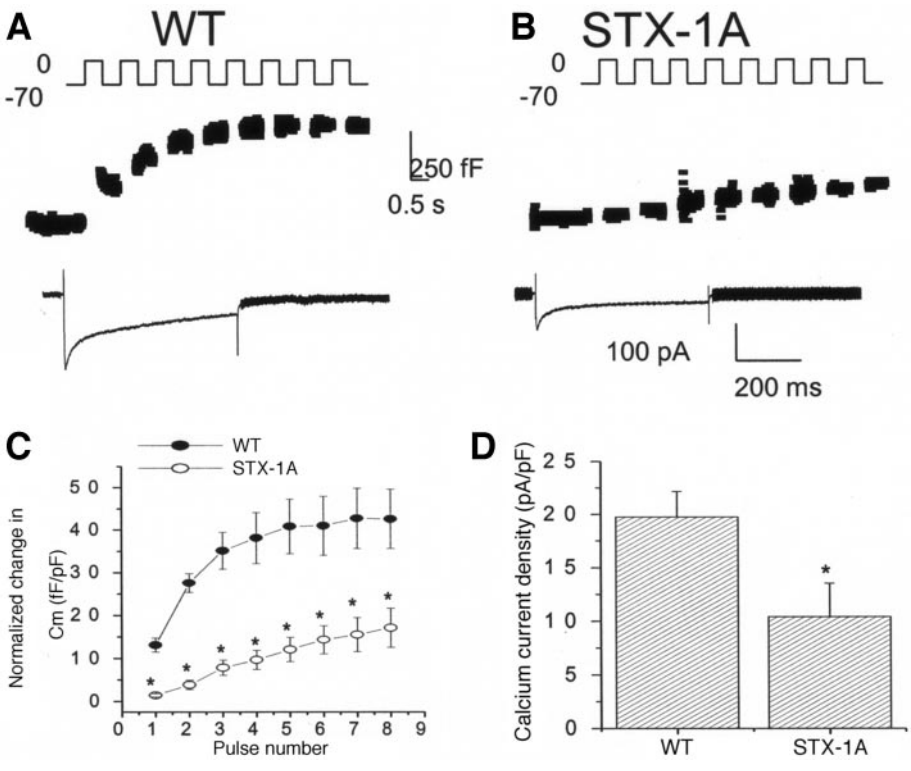

FIG. 6. STX-1A mouse β-cells exhibited reduced exocytosis and Ca^{2+} currents compared with wild-type (WT) mouse β-cells (simultaneous measurement of exocytosis and Ca^{2+} currents). *A* and *B*: Increases of Cm triggered by a train of eight 500-ms depolarizing pulses (1-Hz stimulation frequency) from −70 to 0 mV in control and STX-1A mouse β-cells (*top traces*). *Bottom traces* show the Ca^{2+} currents triggered in the same cells. *C*: The change in Cm is normalized to cell size and plotted against the pulse number. *D*: The results for Ca^{2+} currents are summarized. All values are means ± SE of five to six cells. $*P < 0.05$ compared with wild-type control.

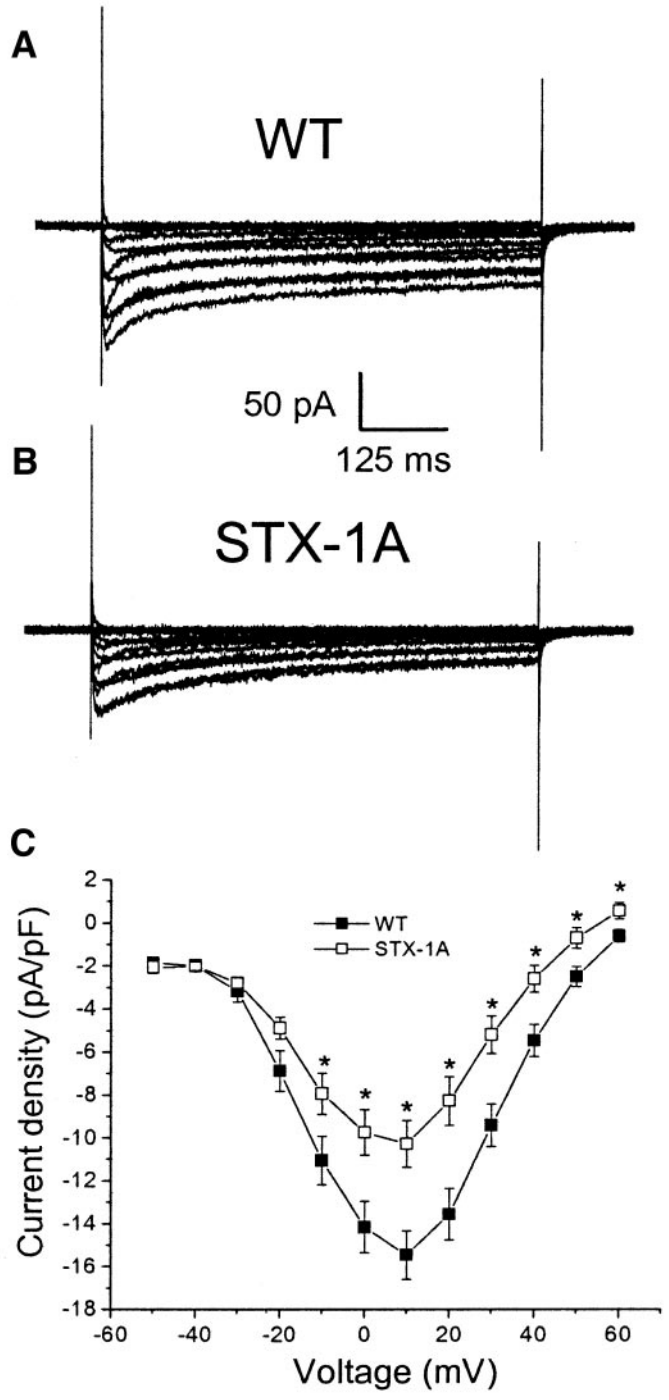

FIG. 7. STX-1A mouse β-cells have reduced voltage-operated Ca^{2+} current density. Ca^{2+} currents are triggered in wild-type (WT; *A*) and STX-1A mouse β-cells (*B*) when the cells are held at −70 mV and then stimulated by increasing depolarizing voltage steps (500 ms) from −50 to +60 mV at 10-mV increments. *C*: Currents are normalized to cell size and plotted against voltage. All values are means ± SE of seven to eight cells. **P* < 0.05 compared with wild-type control.

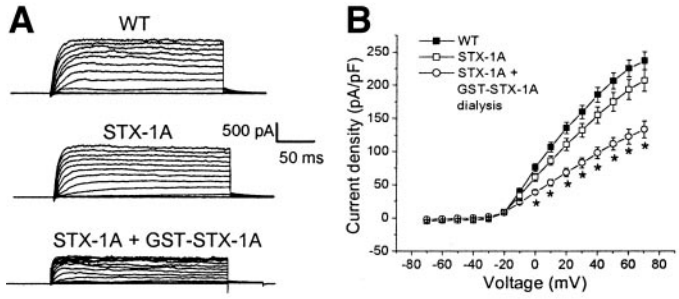

FIG. 8. STX-1A mouse β-cells have K_v channel densities comparable with those of wild-type (WT) mouse β-cells. *A*: Wild-type and STX-1A mouse β-cells were held at −70 mV and then stimulated by increasing depolarizing voltage steps (200 ms) from −70 to +70 mV at 10-mV increments to trigger K_v currents (*top* and *middle traces*). The *bottom trace* shows the K_v currents in STX-1A mouse β-cells dialyzed with 1 μmol/l GST-STX-1A fusion protein for 6 min. *B*: The currents are normalized to cell size and plotted against voltage. All values are means ± SE of 10–17 cells. **P* < 0.05 compared with wild-type control and STX-1A groups.

these tissues might be due to secondary defects of neural and hormonal release (cortisol, catecholamines, and growth hormone) mechanisms, and perhaps even islet α-cell glucagon release. Because these neural and endocrine (i.e., pituitary and adrenal glands and islet α-cells) tissues are also regulated by STX-1A, they would likely also be affected by the overexpression of STX-1A, which could possibly cause abnormal hormone release and in turn influence not only insulin sensitivity of the peripheral tissues but also β-cell insulin secretion as well. Of note, the abnormal insulin sensitivity was manifested only in the male STX-1A mice and not the female STX-1A mice. This suggests an even more important role of the sex hormones, either a favorable influence by female hormones (i.e., estrogens and progesterone) or unfavorable influence by male hormones (i.e., testosterone) on insulin sensitivity of the peripheral tissues. The release of male and female hormones might also be affected by STX-1A either directly or via the STX-1A–mediated neurohormonal (i.e., pituitary-adrenal) release pathways.

The increase in STX-1A levels produced in these mice are well within the range of the effects of polymorphic changes within regulatory elements seen for other genes and so are physiologically relevant. The factor VII locus contains five common polymorphisms that influence circulating levels of factor VII: three within the promoter, one intronic, and one coding (30). Together, these polymorphisms account for close to one-half of the variation in protein levels seen between individuals and appear to have a clinical effect because they can act as either risk or protective factors for myocardial infarction (31,32). Similar polymorphisms that produce modest changes in STX-1A protein levels may also exist in the general population and alter individuals' susceptibility to glucose intolerance or diabetes. We had previously shown that type 2 diabetic rodent models exhibited reduced levels of SNARE proteins in the pancreatic islets, including STX-1A (10). This may also be an underlying mechanism contributing to diabetes in humans. The extremely high frequency of abnormal glucose tolerance reported in adults with WBS, far higher than adults in the general population with similar BMIs (15), strongly suggests an underlying genetic cause, presumably the dominant effect of the deletion of one or more genes within the WBS region. We had postulated that hemizygosity for STX-1A may be a primary cause of abnormal glucose metabolism and neurological abnormalities in WBS (16), raising the possibility that STX-1A could be a diabetogene (33). The effects on glucose metabolism from only a moderate change in STX-1A protein levels seen in our transgenic mouse model indicate that the pancreatic β-cells may be exquisitely

sensitive to such alterations. We postulated that increasing or decreasing the levels of STX-1A within the β-cells may disrupt the proper assembly or function of the insulin exocytotic machinery, either through changing the stoichiometry of the SNARE complex itself or perhaps by altering its interaction with Munc18a. Elucidation of the precise components of the insulin secretory machinery that are altered by a reduced level of STX-1A awaits the generation of mice that are hemizygous for STX-1A.

Our results, demonstrating that small fluctuations of STX-1A levels could profoundly affect ion channels and exocytosis, are of broader relevance to a number of neurological diseases (besides WBS, above) in which the cellular levels of STX-1A are also severely perturbed. The frontal cortexes of patients with schizophrenia and depression whose cause of death was suicide were noted to exhibit elevated STX-1A levels compared with patients who died of other causes (34). These reports taken together suggest that abnormalities in STX-1A levels, either an excess or a deficit, along with the complexes formed with its interacting proteins (ion channels and exocytic proteins) could provide the molecular substrates for abnormalities of neural connectivity, perhaps as a result of the formation of abnormal "nonfunctioning" excitosome complexes (22). In summary, our work demonstrates that even slight fluctuation of islet STX-1A (and presumably other cognate SNARE proteins) levels could contribute to the changing patterns of insulin secretory responses in health and in type 2 diabetes.

ACKNOWLEDGMENTS

H.Y.G. and L.R.O. have received Canadian Diabetes Association Grant 1630 and Canadian Institutes for Health Research Grant CIHR MOP-64465. P.P.L.L. has received a Canadian Institutes for Health Research-Canadian Digestive Health Foundation Graduate Studentship; and Y. Leung has received a postdoctoral fellowship from the Canadian Diabetes Association.

We thank Peter Pasceri for technical assistance in generating the STX-1A mice.

REFERENCES

1. Daniel S, Noda M, Straub SG, Sharp GWG: Identification of the docked granule pool responsible for the first phase of glucose-stimulated insulin secretion. *Diabetes* 48:1686–1690, 1999
2. Rorsman P, Renstrom E: Insulin granule dynamics in pancreatic β-cells. *Diabetologia* 46:1029–1045, 2003
3. MacDonald PE, Wheeler MB: Voltage-dependent K(+) channels in pancreatic beta cells: role, regulation and potential as therapeutic targets. *Diabetologia* 8:1046–1062, 2003
4. Yang S-N, Larsson O, Bränström R, Bertorello AM, Leibiger B, Leibiger IB, Moede T, Köhler T, Meister B, Berggren P-O: Syntaxin interacts with the L_D subtype of voltage-gated Ca^{2+} channels in pancreatic β cells. *Proc Natl Acad Sci U S A* 96:10164, 1999
5. Kang YH, Huang XH, Pasyk EA, Ji J, Holz H, Wheeler MB, Tsushima R, Gaisano HY: Syntaxins-3 and -1A inhibit L-type calcium channel activity, insulin biosynthesis and exocytosis in beta-cell lines. *Diabetologia* 45:231–241, 2002
6. Pasyk E, Kang Y, Huang X, Cui N, Sheu L, Gaisano HY: SNARE binds the nucleotide binding folds of pancreatic islet beta cell sulfonylurea receptor to regulate the K_{ATP} channel. *J Biol Chem* 279:4234–4240, 2004
7. Leung YM, Kang YH, Gao X, Xia F, Xie H, Sheu L, Tsuk S, Lotan I, Tsushima R Gaisano HY: Syntaxin 1A binds to the cytoplasmic C-terminus of Kv2.1 to regulate channel gating and trafficking. *J Biol Chem* 278:17532–17538, 2003
8. Leung Y-M, Kang Y, Xia F, Sheu L, Gao X, Xie H, Tsushima RG, Gaisano HY: Open form syntaxin-1A is more potent than the wild type form in inhibiting Kv2.1 channel: implications for membrane potential regulation in exocytosis. *Biochem J* 387:195–202, 2005
9. Chan CB, MacPhail RM, Sheu L, Wheeler M, Gaisano HY: β-Cell hypertrophy in fa/fa rats is associated with basal glucose hypersensitivity and reduced SNARE protein expression. *Diabetes* 48:997–1005, 1999
10. Gaisano HY, Ostenson C-G, Sheu L, Wheeler WB, Efendic S: Abnormal expression of pancreatic islet exocytotic SNARE proteins in GK rats is partially restored by phlorizin treatment. *Endocrinology* 143:4218–4226, 2002
11. Sheu L, Pasyk EA, Ji J, Huang X, Gao X, Varoqueaux F, Brose N, Gaisano HY: Regulation of insulin exocytosis by Munc13-1. *J Biol Chem* 278:27556–27563, 2003
12. Ohara-Imaizumi M, Nishiwaki C, Kikuta T, Nagai S, Nakamichi Y, Nagamatsu S: TIRF imaging of docking and fusion of single insulin granule motion in primary rat pancreatic beta-cells: different behaviour of granule motion between normal and Goto-Kakizaki diabetic rat beta-cells. *Biochem J* 381:13–18, 2004
13. Nagamatsu S, Nakamichi Y, Yamamura C, Matsushima S, Watanabe T, Ozawa S, Furukawa H, Ishida H: Decreased expression of t-SNARE, syntaxin-1 and SNAP-25 in pancreatic beta cells is involved in impaired insulin secretion from diabetic GK rat islets, restoration of decreased t-SNARE proteins improves impaired insulin secretion. *Diabetes* 48:2367–2373, 1999
14. Nagamatsu S, Fujiwara T, Nakamichi Y, Watanabe T, Katahira H, Sawa H, Akagawa K: Expression and functional role of syntaxin 1/HPC-1 in pancreatic beta cells: syntaxin 1A, but not 1B, plays a negative role in regulatory insulin release pathway. *J Biol Chem* 271:1160–1165, 1996
15. Cherniske E, Carpenter TO, Klaiman C, Young E, Bregman J, Insogna K, Schultz RT, Pober BR: Multisystem study of 20 older adults with Williams syndrome. *Am J Med Genet* 131:255–264, 2004
16. Osborne LR, Soder S, Shi XM, Pober B, Costa T, Scherer SW, Tsui LC: Hemizygous deletion of the syntaxin 1A gene in individuals with Williams syndrome. *Am J Hum Genet* 61:449–452, 1997
17. Expert Committee on the Diagnosis and Classification of Diabetes Mellitus: Report of the Expert Committee on Diagnosis and Classification of Diabetes Mellitus. *Diabetes Care* 22 (Suppl. 1):S5–S19, 1999
18. Ellis J, Talbot D, Dillon N, Grosveld F: Synthetic human beta-globin 5′HS2 constructs function as locus control regions only in multicopy transgene concatamers. *EMBO J* 12:127–134, 1993
19. Gerber SH, Sudhof TC: Molecular determinants of regulated exocytosis. *Diabetes* 51 (Suppl. 1):S3–S11, 2002
20. Zhang W, Efanov A, Yang SN, Fired G, Kolare S, Brown H, Zaitsev S, Berggren PO, Meister B: Munc18 associates with syntaxin and serves as a negative regulator of exocytosis in the pancreatic β-cell. *J Biol Chem* 275:41521–41527, 2000
21. Thurmond DC, Pessin JE: Molecular machinery involved in the insulin-regulated fusion of GLUT4-containing vesicles with the plasma membrane. *Mol Membr Biol* 18:237–245, 2001
22. Wiser O, Trus M, Hernandez A, Renstrom E, Barg S, Rorsman P, Atlas D: The voltage sensitive Lc-type calcium channel is functionally coupled to the exocytotic machinery. *Proc Natl Acad Sci U S A* 96:248–253, 1999
23. Barg S, Ma X, Eliasson L, Galvanovskis J, Gopel SO, Obermuller S, Platzer J, Renstrom E, Trus M, Atlas D, Striessnig J, Rorsman P: Fast exocytosis with few Ca (2+) channels in insulin-secreting mouse pancreatic B cells. *Biophys J* 81:3308–3323, 2001
24. Cui N, Kang Y, He Y, Leung Y-M, Pasyk E, Xie H, Gao X, Sheu L, Hansen JB, Wahl P, Tsushima RG, Gaisano HY: H3 Domain of syntaxin 1A inhibits sulfonylurea receptor 1/K_{ATP} channels by its actions on nucleotide-binding folds-1 and -2. *J Biol Chem* 279:53259–53265, 2004
25. Wiser O, Bennett MK, Atlas D: Functional interaction of syntaxin and SNAP-25 with voltage-sensitive L- and N-type Ca^{2+} channels. *EMBO J* 15:4100–4110, 1996
26. Michaelevski I, Chikvashvili D, Tsuk S, Singer-Lahat D, Kang Y, Linial M, Gaisano HY, Fili O, Lotan I: Direct interaction of t-SNAREs with the Kv2.1 channel: modal regulation of channel activation and inactivation gating. *J Biol Chem* 278:34320–34330, 2003
27. Tsuura Y, Ishida H, Okamoto Y, Kato S, Sakamoto K, Horie M, Ikeda H, Okada Y, Seino Y: Glucose sensitivity of ATP-sensitive K+ channels is impaired in beta-cells of the GK rat: a new genetic model of NIDDM. *Diabetes* 42:1446–1453, 1993
28. Weimer RM, Jorgensen EM: Controversies in synaptic vesicle exocytosis. *J Cell Sci* 116:3661–3666, 2003
29. Dulubova I, Sugita S, Hill S, Hosaka M, Fernandez I, Sudhof TC, Rizo J: A conformational switch in syntaxin during exocytosis, a role of Munc18. *EMBO J* 18:4372–4382, 1999
30. Lane DA, Grant PJ: Role of hemostatic gene polymorphisms in venous and arterial thrombotic disease. *Blood* 95:1517–1532, 2000

31. Girelli D, Russo C, Ferraresi P, Olivieri O, Pinotti M, Friso S, Manzato F, Mazzucco A, Bernardi F, Corrocher R: Polymorphisms in the factor VII gene. *N Engl J Med* 343:774–780, 2000
32. Bozzini C, Girelli D, Bernardi F, Ferraresi P, Olivieri O, Pinotti M, Martinelli N, Manzato F, Friso S, Villa G, Pizzolo F, Beltrame F, Corrocher R: Influence of polymorphisms in the factor VII gene promoter on activated factor VII levels and on the risk of myocardial infarction in advanced coronary atherosclerosis. *Thromb Haemost* 92:541–549, 2004
33. Tsunoda K, Sanke T, Nakagawa T, Furuta H, Nanjo K: Single nucleotide polymorphism (D68D, T to C) in the syntaxin 1A gene correlates to age at onset and insulin requirement in type II diabetic patients. *Diabetologia* 44:2092–2097, 2001
34. Honer WG, Falkai P, Bayer TA, Xie J, Hu L, Li H-Y, Arango V, Mann JJ, Dwork AJ, Trimble W S: Abnormalities of SNARE mechanism proteins in anterior frontal cortex in severe mental illness. *Cereb Cortex* 12:349–356, 2002